

Electrical Properties and Structure of Cr-Doped Nonstoichiometric V_2O_3 *

H. KUWAMOTO AND J. M. HONIG

Department of Chemistry, Purdue University, West Lafayette, Indiana 46907

Received March 5, 1979; in revised form July 2, 1979

The effect of oxygen nonstoichiometry has been investigated for Cr-doped V_2O_3 . Both high-temperature and low-temperature electrical transitions are gradually suppressed by excess oxygen content. At levels $\delta = 0.04$ for $(V_{0.99}Cr_{0.01})_2O_{3+\delta}$ the transitions disappear completely, and only metallic properties are encountered. The results are interpreted in terms of possible mechanisms for the two metal-insulator transitions encountered in Cr-doped V_2O_3 .

Introduction

Vanadium oxides have been extensively investigated because they show many striking variations in their electrical properties (1). For example, V_2O_3 doped with 1 atom% Al_2O_3 or Cr_2O_3 exhibits two sharp electrical transitions: one in the range 150–190 K (T_1) and a second, near room temperature (T_2) (2, 3). At T_1 the transition is accompanied by the onset of magnetic order and by a concomitant change in symmetry (4). By contrast, the T_2 transition from metallic ($T < T_2$) to insulating ($T > T_2$) character is not accompanied by an alteration in crystal symmetry (5): however, the lattice parameters and interatomic distances change discontinuously (2, 5).

Single crystals used in such studies have been prepared principally through three techniques: pulling crystals from the melt (6–8), use of flux methods (2, 9), and chemical vapor transport (CVT) techniques (10–14). By employing CVT, Pouchard and Launay (12) obtained nonstoichiometric

V_2O_3 using $TeCl_4$ as the transport agent. The effects of altering growth conditions on the quality of V_2O_3 crystals have been investigated by Peshev *et al.* (13) and by Launay and co-workers (14). As the conditions for obtaining high-quality single crystals they cited: the use of a relatively small amount of $TeCl_4$, maintenance of a small temperature gradient between the regions of the furnace where evaporation and growth take place, and use of V_2O_3 powder which is slightly deficient in oxygen.

In this paper, we report on two aspects of the V_2O_3 problem which have not been discussed heretofore: (i) the effect of changing conditions in chemical vapor transport techniques on the crystal morphology, and (ii) electrical properties in nonstoichiometric chromium-doped V_2O_3 grown by chemical vapor transport techniques.

Experimental

The V_2O_5 powder was first reduced to V_2O_3 in a H_2 atmosphere at 1000°C. The resulting V_2O_3 in pure form, or containing appropriate amounts of Cr_2O_3 as starting

* Research supported by NSF/MRL Grants DMR76-00889A01 and DMR77-23798.

powder, was sealed off at a pressure $p \approx 10^{-5}$ Torr in a 15-mm-i.d. \times 180-mm-long quartz tube with various amounts of powdered TeCl_4 which was used as the transport agent. Crystal growth runs were carried out in a horizontal kanthal furnace. The temperature of the cooling zone was always maintained at roughly 950°C ; the hot zone temperatures and the amounts of TeCl_4 used in the various runs are displayed in Fig. 2. In all experiments the sealed quartz tubes were kept in the furnace for 6 days. The starting powder normally deviated from the exact 3:2 oxygen:metal stoichiometry; the final δ value in $(\text{V}_{1-x}\text{Cr}_x)_2\text{O}_{3+\delta}$ was governed by the moisture content and the quantity of TeCl_4 used for vapor transport, and by the composition of the starting mixture, i.e., by the V/O ratio.

The stoichiometry of the resulting single crystals was determined by reoxidation to V_2O_5 in a platinum boat at 670°C , slightly below the melting point of V_2O_5 . The heating process in flowing oxygen was maintained for 1 week; this condition was chosen after repeating the oxidation and weighing processes in steps of 1 day until no further mass change was detected. No direct Cr analysis was performed on these samples, but such chemical analyses were performed on stoichiometric $(\text{V}_{1-x}\text{Cr}_x)_2\text{O}_3$ grown from the melt where a close match between actual and nominal Cr content was found in all cases.

Samples grown from the melt and by CVT techniques yielded resistivities that were virtually identical; since electrical properties are a very sensitive function of Cr content, the nominal and actual x values in the current group of CVT-grown specimens must also correspond closely. However, even if the nominal Cr content in the present investigation were in error by 100% the resulting change in δ would be less than the experimental error whose magnitude is shown by the number of significant figures quoted in Table I.

The resulting crystals were examined by X-ray powder diffraction technique, using nickel-filtered $\text{CuK}\alpha$ radiation. The lattice parameters were determined from 2θ values of nine reflections by least-squares techniques. This calculation is based on a linear extrapolation of a plot of d versus $\cot\theta$ to $\theta = 90^\circ$. This may be used to correct for a constant calibration error persisting at $2\theta = 180^\circ$.

Resistivity measurements were carried out with the standard four-probe technique in a gettered helium gas atmosphere.

Morphology and Crystal Growth Conditions

Some crystals obtained by chemical vapor transport techniques are shown in Fig. 1; both needle-like or polyhedron-like habits are identifiable. These crystals dimensions

TABLE I
LATTICE PARAMETERS (\AA) FOR $(\text{V}_{1-x}\text{Cr}_x)_2\text{O}_{3+\delta}$ AT ROOM TEMPERATURE

Unit cell parameter	Compound			
	$(\text{V}_{0.99}\text{Cr}_{0.01})_2\text{O}_3$	$(\text{V}_{0.99}\text{Cr}_{0.01})_2\text{O}_{3.02}$	$(\text{V}_{0.99}\text{Cr}_{0.01})_2\text{O}_{3.03}$	$(\text{V}_{0.97}\text{Cr}_{0.03})_2\text{O}_{3.05}$
Metallic phase				
a	4.954	4.956 ± 0.002	4.957 ± 0.002	
c	13.99	13.99 ± 0.01	14.00 ± 0.01	
Insulating phase				
a	4.997			4.989 ± 0.004
c	13.926			13.92 ± 0.01

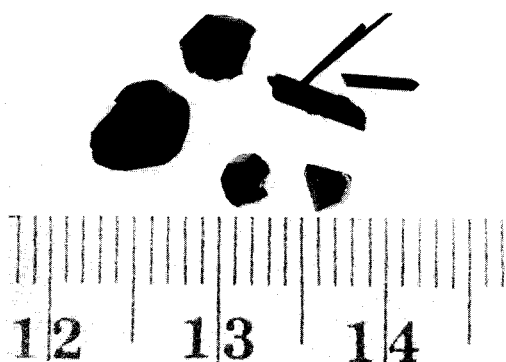


FIG. 1. Several types of V_2O_{3+8} single crystals grown by CVT. Scale in centimeters and millimeters.

ranged up 10 mm on a side. No difference in crystallographic characteristics was encountered between V_2O_3 and Cr-doped V_2O_3 .

A number of factors are thought to affect the morphology, among them: the impurity content of the starting material, the growth rate, and the deposition temperature. In equilibrium with its surroundings a crystal minimizes its surface free energy so that the equilibrium shape of the crystal is bounded by the so-called Wulff plot based on Wulff's theorem (15). Crystal growth requires a departure from equilibrium conditions which permit alterations in the shape of the crystal. If impurities are adsorbed on the crystal surface, the crystal habit is also altered from its equilibrium shape. An attempt was therefore made to eliminate gross impurity effects, by use of the same quality starting materials at the beginning of each run. Also, since $TeCl_4$ is very hygroscopic moisture could well affect the crystal morphology; however, no such effects were detected when $TeCl_4$ was allowed to absorb moisture from atmosphere for various lengths of time prior to a run.

Finally, changes in stoichiometry were examined: According to the literature (11), growth of V_2O_3 single crystals requires the presence of some excess VO or V in the starting material. We examined the effect of slight variations in stoichiometry achieved by altering the VO or V content; the

morphology of V_2O_3 remained unaffected by such variations.

The relation between growth conditions and the resulting morphology of V_2O_3 is illustrated in Fig. 2. It is seen that the growth temperature and rate do affect the morphology of V_2O_3 ; this is also the case for Cr-doped V_2O_3 . On decreasing the amount of transport agent as well as the hot zone temperature (i.e., by reducing the growth rate), the crystal morphology tends toward plate-like rather than needle-like crystals. From the Laue diffraction patterns the large facet of the plate-like crystals in Fig. 1 was shown to be the $\{001\}$ plane, and the growth axis of the needle-like crystals was found to be along the $\langle 001 \rangle$ direction. This suggests that the growth rate along the $\langle 001 \rangle$ direction decreases with the crystal growth rate. It is also known that the most stable surface configuration is altered with changes in the supersaturated pressure of the vapor. When the amount of $TeCl_4$ was reduced so that the vapor pressure of the starting material and the crystal growth rate might be decreased, extremely thin plates were obtained. For crystals deposited in the cooling zone, the $\{001\}$ planes for the plate-like crystals were found to be aligned parallel to the temperature gradient, i.e., along the axis of

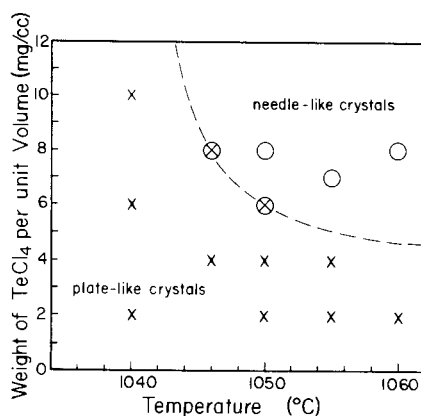


FIG. 2. Morphology changes obtained by alteration of the amount of transport agent and by changes in the hot zone temperature.

the tube; on the other hand, the $\langle 001 \rangle$ directions of a long growth axis of the needle-like crystals were from 0 to 45° away from the axis of the temperature gradient. These features agree quite well with the very limited data reported by Peshev *et al.* (13). In their paper only the effects of altering the temperature gradient at one fixed concentration of TeCl_4 were reported; also, they investigated the results achieved by altering the amount of transport agent at only one fixed zone temperature. Figure 2 is a generalization of their work.

Launay *et al.* (14) suggested that use of smaller amounts of TeCl_4 improves the quality of grown crystals; however, we were unable to confirm this observation. We did find that slow crystal growth with small amounts of TeCl_4 yields larger crystals; in that sense, the use of minimal amounts of TeCl_4 is recommended.

Resistivity and Lattice Parameter Measurements

Electrical resistivity measurements for several Cr-doped V_2O_3 samples grown by chemical vapor transport techniques are

presented in Fig. 3, along with their chemical compositions. There was no clearcut difference in electrical properties between stoichiometric crystals grown by the present technique and those grown from the melt (16, 17). For stoichiometric Cr-doped V_2O_3 the temperature range of stability for the metallic phase narrows with increasing chromium content; however, the size of the resistivity discontinuity accompanying the high-temperature transition at T_2 does not change significantly (17). Curves (b)–(f) show that the $(\text{V}_{0.99}\text{Cr}_{0.01})_2\text{O}_{3+\delta}$ alloys become increasingly metallic as the oxygen excess δ is increased. With increasing deviations from strict stoichiometry the high-temperature transition at $T = T_2$ disappears and the metal–antiferromagnetic insulator transition at $T = T_1$ is shifted to lower temperatures and ultimately is also eliminated. This was checked by carrying out resistivity measurements down to 4.2 K. The hysteresis effects were independent of δ and were in excess of 50 K for the high-temperature transition and the range 7–10 K for the low-temperature transition. The changes in transition with δ are very abrupt; the two samples (e) and (f) of nominally identical

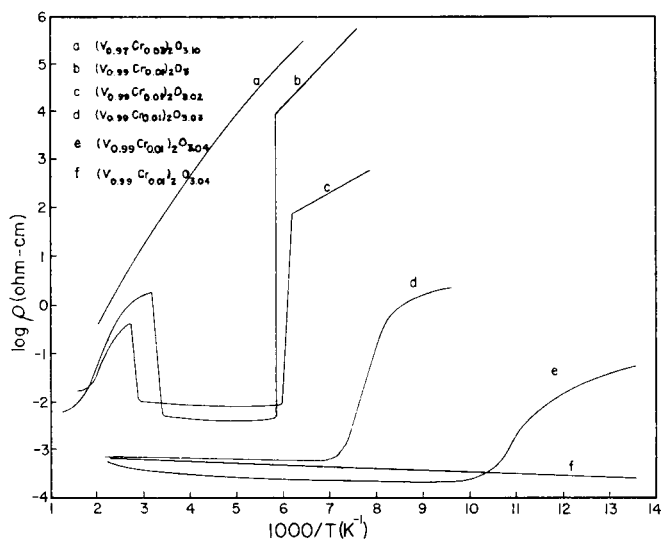


FIG. 3. Resistivity vs $1/T$ for several nonstoichiometric Cr-doped V_2O_3 single crystals.

composition, $x = 0.01$ and $\delta = 0.04$, exhibit quite different behavior at temperatures below 100 K. The rather large temperature range over which the metal–antiferromagnetic insulator transition takes place suggests a rather severe nonuniformity in oxygen excess content in the samples under study.

Table I shows that the a and c lattice parameters of the metallic phase for 1% Cr-doped V_2O_3 , as determined by X-ray diffraction at room temperature, remain almost unaffected by departures from stoichiometry. This immediately suggests that the high-temperature transition which disappears in the range of δ under study is not tied to any changes in atomic configuration of the metallic phase. In ongoing, parallel experiments we have similarly shown (18) that the lattice parameters for $(V_{0.99}M_{0.01})_2O_3$ with $M = Al, Cr, Fe, Ga, Rh,$ and Ti are nearly identical. The fact that among all of these only Al- and Cr-doped V_2O_3 exhibit the high-temperature transition (3, 17, 18) supports the feature described above, i.e., that the lattice parameter does not play a critical role in the high-temperature transition.

The results obtained here are comparable to those reported by prior investigators (3, 11, 14, 19, 20–22) for a variety of undoped crystals of $V_2O_{3+\delta}$. These studies involved measurements of magnetic susceptibility (3, 11), resistivity (3, 14, 19), positron lifetime (21), and Mössbauer resonance (22). In all cases there seems general agreement that excess oxygen at levels $\delta \approx 0.04$ suffices to suppress both the high-temperature anomaly and the low-temperature transition encountered in pure V_2O_3 .

Discussion

Close examination of the above data reveals several interesting features: As has already been stated, the replacement of V by Cr tends to render V_2O_3 more insulating, witness the gradual reduction in stability of

the metallic (M) against the insulating (I) and antiferromagnetic insulator (AFI) phases, and the ultimate disappearance of the M phase with sufficient Cr doping. This process can be partially reversed by rendering Cr-doped V_2O_3 nonstoichiometric. As is shown in Fig. 3 for 1 atom% Cr-doped V_2O_3 , the incorporation into the host lattice of excess oxygen counteracts the effect of Cr-doping, by widening the stability range of the M phase and then eliminating first the I and then the AFI phases. It is remarkable that the trend toward insulating effects achieved by Cr substitution in the cation sublattice may be counteracted by changes involving the anion sublattice. This is complementary to the fact, noted previously (17), that oxygen incorporation has qualitatively the same effect on V_2O_3 as the use of Ti; here either anion or cation sublattice substitution achieves similar results.

A parallel effect is also evident in the transition temperature T_1 at which the M phase gives way to the AFI phase on cooling. No sharp transition temperature is actually discernible for the higher oxygen content δ in Fig. 3, but for the qualitative comparisons made here it suffices to take the midpoint of the electrical transition as an indicator of T_1 . It is then found that T_1 for $(V_{0.99}Cr_{0.01})_2O_{3+\delta}$ lies well above the scatter of transition temperatures T_1 reported in the literature for undoped $V_2O_{3+\delta}$, summarized in Fig. 4. This indicates that for Cr-doped V_2O_3 a greater deviation δ from stoichiometry is required to reach a given T_1 than for undoped V_2O_3 , as would be anticipated from the preceding discussion.

One should note, however, that the effects achieved by heavy Cr doping cannot be counteracted by use of excess oxygen. This is evident by examining curve (a) in Fig. 3 for $(V_{0.97}Cr_{0.03})_2O_{3.10}$. In stoichiometric V_2O_3 the use of 2 atom% Cr eliminates the M phase altogether; one has, instead, only a residual AFI– I transition near 170 K. Curve (a) fails to show this residual change as well as

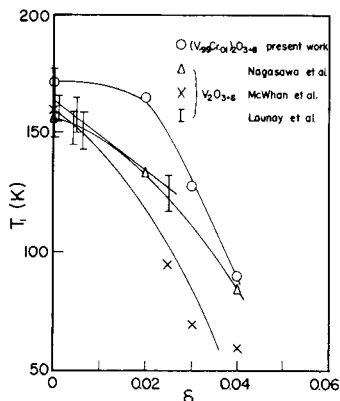


FIG. 4. Transition temperature (T_1) vs oxygen excess, δ .

the restoration of metallic characteristics at such heavy doping levels with Cr and O.

The quantity $\Delta \equiv 2x - f\delta$ determines whether a given alloy $(V_{1-x}Cr_x)_2O_{3+\delta}$ undergoes a transition or not; here f is a parameter that must be estimated. If $\Delta > 0.005$ the above alloy undergoes the high-temperature transition, but if $\Delta < 0.005$ the alloy remains metallic up to highest temperature. We estimate the f parameter for oxygen doping to be $f = 0.7-1$, on the basis that curve (c) of Fig. 3 is quite similar to the variation of $\log \rho$ vs T^{-1} for $(V_{1-\Delta}Cr_{\Delta})_2O_3$, where $\Delta = 0.006$ (17). For $\delta > 0.015$, there is no high-temperature transition in Fig. 3; the low-temperature transition disappears for $\delta > 0.04$.

The difference between $V_2O_{3+\delta}$ and $(V_{0.99}Cr_{0.01})_2O_{3+\delta}$ is evident from Table I: in Cr-doped nonstoichiometric V_2O_3 both the a and c lattice parameters of the metallic phase remain essentially unaffected by incorporation of excess oxygen. Since it is known that changes in bond distances are always accompanied by alterations in lattice parameters (5), the approximate constancy of a and c indicates that neither the V-V nor the V-O distances are greatly altered by variations in δ . Even the transition to the insulating phase changes the lattice parameters by less than 0.05 and 0.07 Å along a_H and c_H , respectively; the lattice

parameters of the insulating phase are likewise little affected by deviations from stoichiometry. By contrast, for undoped $V_2O_{3+\delta}$ both a_H and c_H diminish appreciably with increased δ (3, 11). We cannot at this time provide an explanation for the above difference in properties. It is highly unlikely that we were dealing with a multiphase system: Neither careful examination by optical microscopy nor the X-ray diffraction experiments showed any evidence of multiphase properties. Also, it is very difficult to understand the changes in electrical properties displayed in Fig. 3 on the basis of physical inhomogeneities in the crystal structure rather, it is necessary to postulate gradation in homogeneous properties to explain the results. In both undoped and Cr-doped nonstoichiometric V_2O_3 the ratio c_H/a_H remains fixed at a value of 2.83, independent of the deviation from stoichiometry, in the metallic range. For the insulating phase this ratio drops to 2.79. The reason that both ratios could be determined at room temperature is that, as has been observed (17, 18) for stoichiometric $(V_{1-x}Cr_x)_2O_3$ with $0.005 \leq x \leq 0.0179$, there is an enormous hysteresis loop centered around room temperature which separates the $M-I$ transition in the heating and cooling cycles.

The situation with respect to resistivity changes for $V_2O_{3+\delta}$ at T_2 is unclear at present: McWhan and co-workers (3) working with pressed powders, reported no change in the magnitude of the resistivity discontinuity at T_2 with δ . By contrast Nagasawa *et al.* (11) reported a gradual reduction of the resistivity discontinuity with increasing δ for single-crystal specimens. Our own observations on Cr-doped nonstoichiometric V_2O_3 fall more nearly in line with the findings of Nagasawa *et al.* however, the resistivity of $V_2O_{3+\delta}$ in the metallic phase, as reported in Ref. (11) increased dramatically with δ , whereas it varied only very weakly with δ in the measurements displayed in Fig. 3.

The fact that the drastic changes in electrical characteristics depicted in Fig. 3 can be brought about without large alterations in the lattice shows once more that one is not dealing here with phenomena which depend on changes in relative atomic positions. This particular observation weakens earlier contentions that the high-temperature phase change is a manifestation of the Mott transition (2). Were this the case one would anticipate a critical lattice spacing above which the transition would take place. These remarks obviously do not invalidate other mechanisms that can be used to bring about a metal-insulator transition, such as the use of pressure (23) to force a reduction in bond distances, thus stabilizing the metallic phase.

The above findings may, however, be brought into a consistent pattern with the assumption that a deep minimum exists in the density of states (DOS) for V_2O_3 which is intersected by the Fermi level. Such a model has recently been proposed (24) to interpret the effects of Cr doping on the electrical properties of V_2O_3 . This type of DOS is consistent with recent calculations by Castellani *et al.* (25) as well as earlier work by Ashkenazi, Weger, and collaborators (26–28). Prior experiments (17) had shown that incorporation of 1.78 atom% Cr into V_2O_3 increases the resistivity of the metallic phase of V_2O_3 from $\rho \approx 2 \times 10^{-4}$ to $\rho \approx 3 \times 10^{-2}$ ohm-cm. Such an enormous jump, coupled to a virtually constant value of the Seebeck coefficient in this doping range, is consistent with the concept (29) that substitution of Cr for V tends to widen all valleys and to increase the peak heights. If this is so then with incorporation of Cr the minimum in the DOS progressively deepens, resulting in a corresponding increase of the resistivity of the metallic phase. Ultimately, for $x > 0.018$ a gap opens up in the DOS, and the metallic state disappears altogether.

One can now anticipate two effects resulting from incorporation of excess oxygen. First, holes are introduced into the manifold

of primarily $3d$ -type character. This depresses the Fermi level, so that only states in the lower portion of the band are populated. Therefore, as long as the Fermi level drops well below the position of the minimum in the DOS, the nonstoichiometric alloy system will revert to the metallic state regardless of the perturbations in the DOS incurred by changes in the Cr content of the system. Second, as vacancies are generated in the cation sublattice due to incorporation of excess oxygen, the V–V interaction, already weakened through the substitution of Cr for V, is further disrupted, thus gradually eliminating antiferromagnetic ordering. This would explain the rapid decline of the Néel temperature with increasing x and/or δ and the ultimate elimination of the AFI phase. Such a model lends credence to the assertion (25) that the monoclinic distortion is a manifestation of magnetostriction accompanying the establishment of antiferromagnetic order.

In this connection it should be noted that a band overlap model which has on occasion been invoked (30, 31) to explain the physical characteristics now seems inappropriate because of the recent finding (24) that the Seebeck coefficient does not track the resistivity variations with Cr content, contrary to theoretical predictions based on the overlap model (24).

Finally, one should be aware of several additional complications: First, no explanation has been offered to account for the properties of $(V_{0.97}Cr_{0.03})_2O_{3.10}$, curve (a) of Fig. 3; the corresponding stoichiometric alloy does not exhibit a range of metallic behavior either but does undergo the I -AFI transition at T_N . Until a more thorough investigation is initiated it remains unclear why oxygen excess fails to suppress the I phase when $x = 0.03$. Second, the transition at T_2 manifested by $(V_{1-x}Cr_x)_2O_3$ alloys is accompanied by various subtle changes in crystal structure, as shown by the detection of weak extra satellite diffraction peaks

(32), which indicate the existence of extra lattice periodicities in the insulating relative to the metallic phase. This feature would assist in the generation of the gap characterizing the properties of the insulator. Third, the effects of electron-phonon interactions have not been properly dealt with.

In summary, we have attempted to explain the electrical characteristics encountered here in terms of the deletion of band states with the deepening of a minimum in the DOS which results ultimately in the generation of a gap when sufficient Cr is incorporated in the lattice. In this model the addition of excess oxygen lowers the position of the Fermi level to restore metallic characteristics, at the same time that the antiferromagnetic order is destroyed because of the generation of vacancies in the cation sublattice.

Acknowledgments

The authors are grateful to Professor H. Sato for helpful discussions on crystal preparation, and to S. A. Shivashankar for his help in low-temperature resistivity measurements.

References

1. See, for example, J. M. HONIG AND L. L. VAN ZANDT, in "Annual Review of Materials Science" (R. Huggins, R. H. Bube, and R. W. Roberts, Eds.), Vol. 5, p. 255, Annual Reviews Inc., Palo Alto, Calif. (1975).
2. D. B. MCWHAN AND J. P. REMEIKA, *Phys. Rev. B* **2**, 3734 (1970).
3. D. B. MCWHAN, A. MENTH, AND J. P. REMEIKA, *J. Phys.* **32**, C1-1079 (1971).
4. P. D. DERNIER AND M. MAREZIO, *Phys. Rev. B* **2**, 3771 (1970).
5. W. R. ROBINSON, *Acta Cryst. B* **31**, 1153 (1975).
6. T. B. REED, *Mater. Res. Bull.* **2**, 349 (1967).
7. T. B. REED AND E. P. POLLARD, *J. Cryst. Growth* **2**, 243 (1968).
8. J. C. C. FAN AND T. B. REED, *Mater. Res. Bull.* **7**, 1403 (1972).
9. D. B. MCWHAN, A. JAYARAMAN, AND J. P. REMEIKA, *Phys. Rev. Lett.* **34**, 547 (1975).
10. K. NAGASAWA, *Mater. Res. Bull.* **6**, 853 (1971).
11. K. NAGASAWA, Y. BANDO, AND T. TAKADA, *J. Cryst. Growth* **17**, 143 (1972).
12. M. POUCHARD AND J. C. LAUNAY, *Mater. Res. Bull.* **8**, 95 (1973).
13. P. PESHEV, G. BLIZNAKOV, G. GYUROV, AND M. IVANOVA, *Mater. Res. Bull.* **8**, 915 (1973).
14. J. C. LAUNAY, M. POUCHARD, AND R. AYROLES, *J. Cryst. Growth* **36**, 297 (1976).
15. G. WULFF, *Z. Krist.* **34**, 449 (1901).
16. A. P. B. SINHA, G. V. CHANDRASHEKHAR, AND J. M. HONIG, *J. Solid State Chem.* **12**, 402 (1975).
17. H. KUWAMOTO, H. V. KEER, J. E. KEEM, S. A. SHIVASHANKAR, L. L. VAN ZANDT, AND J. M. HONIG, *J. Phys.* **37**, C4-35 (1976).
18. H. KUWAMOTO AND J. M. HONIG, to be published; H. KUWAMOTO, thesis, Purdue University (1978).
19. M. NAKAHIRA, S. HORIUCHI, AND H. OOSHIMA, *J. Appl. Phys.* **41**, 836 (1970).
20. V. N. NOVIKOV, B. A. TALLERCHIK, E. I. GINDIN, AND V. G. PROKHVATILOV, *Sov. Phys. Solid State* **12**, 2061 (1971).
21. N. KIMIZUKA, M. ISHII, M. SAEKI, M. NAKANO, AND M. NAKAHIRA, *Solid State Commun.* **12**, 43 (1973).
22. Y. UEDA, K. KOSUGE, S. KACHI, T. SHINJO, AND T. TAKADA, *Mater. Res. Bull.* **12**, 79 (1977).
23. A. JAYARAMAN, D. B. MCWHAN, J. P. REMEIKA, AND P. D. DERNIER, *Phys. Rev. B* **2**, 3751 (1970).
24. H. KUWAMOTO, J. M. HONIG, AND J. APPEL, submitted for publication.
25. C. CASTELLANI, C. R. NATOLI, AND J. RANNINGER, *Phys. Rev. B* **18**, 4945, 4967, 5001 (1978).
26. J. ASHKENAZI AND M. WEGER, *J. Phys. Paris* **37**, C4-189 (1976).
27. J. ASHKENAZI AND T. CHUCHEM, *Phil. Mag.* **32**, 763 (1975).
28. J. ASHKENAZI AND M. WEGER, *Advan. Phys.* **22**, 207 (1973).
29. T. M. RICE AND W. F. BRINKMAN, *Phys. Rev. B* **5**, 4350 (1972).
30. J. B. GOODENOUGH, in "Proceedings of the Tenth International Conference on the Physics of Semiconductors, Cambridge, Massachusetts, 1970" (E. S. P. Keller, J. C. Hensel, and F. Stern, Eds.), p. 304, NSAFC, Division of Technical Information, Materials Technical Information Service, National Bureau of Standards, U.S. Department of Commerce, Springfield, Va.
31. H. ZEIGER, *Phys. Rev. B* **11**, 5132 (1975).
32. F. SINCLAIR AND R. COLELLA, *Solid State Commun.* **31**, 359 (1979).